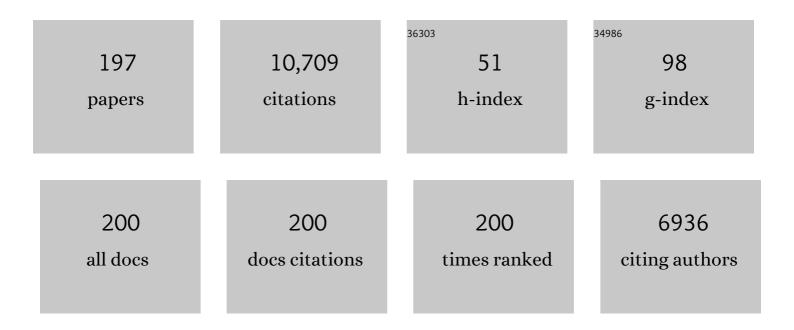
List of Publications by Year in descending order

Source: https://exaly.com/author-pdf/5484432/publications.pdf Version: 2024-02-01



SHUALLENC

#	Article	IF	CITATIONS
1	Improved visualization of the wrist at lower radiation dose with photon-counting-detector CT. Skeletal Radiology, 2023, 52, 23-29.	2.0	26
2	Clinical evaluation of a phantom-based deep convolutional neural network for whole-body-low-dose and ultra-low-dose CT skeletal surveys. Skeletal Radiology, 2022, 51, 145-151.	2.0	11
3	Deepâ€learning model observer for a lowâ€contrast hepatic metastases localization task in computed tomography. Medical Physics, 2022, 49, 70-83.	3.0	7
4	Dependence of Water-equivalent Diameter and Size-specific Dose Estimates on CT Tube Potential. Radiology, 2022, 303, 404-411.	7.3	4
5	First Clinical Photon-counting Detector CT System: Technical Evaluation. Radiology, 2022, 303, 130-138.	7.3	201
6	A New Frontier in Temporal Bone Imaging: Photon-Counting Detector CT Demonstrates Superior Visualization of Critical Anatomic Structures at Reduced Radiation Dose. American Journal of Neuroradiology, 2022, 43, 579-584.	2.4	43
7	Technical note: Evaluation of Artificial 120â€kilovolt computed tomography images for radiation therapy applications. Medical Physics, 2022, , .	3.0	1
8	Improved assessment of coronary artery luminal stenosis with heavy calcifications using high-resolution photon-counting detector CT. , 2022, , .		9
9	Impact of improved spatial resolution on radiomic features using photon-counting-detector CT. , 2022, , .		4
10	A 25-reader performance study for hepatic metastasis detection: lessons from unsupervised learning. , 2022, , .		1
11	Improving coronary artery imaging in single source CT with cardiac motion correction using attention and spatial transformer based neural networks. , 2022, , .		2
12	Quantification of coronary calcification using high-resolution photon-counting-detector CT and an image domain denoising algorithm. , 2022, , .		5
13	Quantitative assessment of motion effects in dual-source dual energy CT and dual-source photon-counting detector CT. , 2022, , .		1
14	Utility of an automatic adaptive iterative metal artifact reduction AiMAR algorithm in improving CT imaging of patients with hip prostheses evaluated for suspected bladder malignancy. Abdominal Radiology, 2022, 47, 2158-2167.	2.1	3
15	Estimating the Clinical Impact of Photon-Counting-Detector CT in Diagnosing Usual Interstitial Pneumonia. Investigative Radiology, 2022, 57, 734-741.	6.2	34
16	Ultra-high-resolution imaging of the shoulder and pelvis using photon-counting-detector CT: a feasibility study in patients. European Radiology, 2022, 32, 7079-7086.	4.5	31
17	A minimum SNR criterion for computed tomography object detection in the projection domain. Medical Physics, 2022, 49, 4988-4998.	3.0	5
18	Characterization of thrombus composition with multimodality CT-based imaging: an in-vitro study. Journal of NeuroInterventional Surgery, 2021, 13, 738-740.	3.3	12

#	Article	IF	CITATIONS
19	Lowâ€dose CT image and projection dataset. Medical Physics, 2021, 48, 902-911.	3.0	89
20	X-Ray Transmittance Modeling-Based Material Decomposition Using a Photon-Counting Detector CT System. IEEE Transactions on Radiation and Plasma Medical Sciences, 2021, 5, 508-516.	3.7	5
21	Photon Counting CT: Clinical Applications and Future Developments. IEEE Transactions on Radiation and Plasma Medical Sciences, 2021, 5, 441-452.	3.7	68
22	Technical Note: kVâ€independent coronary calcium scoring: A phantom evaluation of score accuracy and potential radiation dose reduction. Medical Physics, 2021, 48, 1307-1314.	3.0	10
23	Initial testing of pegfilgrastim (Neulasta Onpro) onâ€body injector in multiple radiological imaging environments. Journal of Applied Clinical Medical Physics, 2021, 22, 343-349.	1.9	1
24	The feasibility of low iodine dynamic CT angiography with test bolus for evaluation of lower extremity peripheral artery disease. Vascular, 2021, 29, 170853812098630.	0.9	0
25	Empirical beam hardening and ring artifact correction for xâ€ray grating interferometry (EBHCâ€GI). Medical Physics, 2021, 48, 1327-1340.	3.0	0
26	High resolution, full field of view, whole body photon-counting detector CT: system assessment and initial experience. , 2021, 11595, .		5
27	Random search as a neural network optimization strategy for Convolutional-Neural-Network (CNN)-based noise reduction in CT. , 2021, 11596, .		10
28	Deep-learning lesion and noise insertion for virtual clinical trial in chest CT. , 2021, 11595, .		0
29	Feasibility of using megavoltage computed tomography to reduce proton range uncertainty: A simulation study. Journal of Applied Clinical Medical Physics, 2021, 22, 131-140.	1.9	2
30	Improved coronary calcification quantification using photon-counting-detector CT: an ex vivo study in cadaveric specimens. European Radiology, 2021, 31, 6621-6630.	4.5	37
31	Deep-learning-based direct synthesis of low-energy virtual monoenergetic images with multi-energy CT. Journal of Medical Imaging, 2021, 8, 052104.	1.5	8
32	Taskâ€specific efficient channel selection and bias management for Gabor function channelized Hotelling observer model for the assessment of xâ€ray angiography system performance. Medical Physics, 2021, 48, 3638-3653.	3.0	1
33	Implementation and experimental evaluation of Mega-voltage fan-beam CT using a linear accelerator. Radiation Oncology, 2021, 16, 139.	2.7	1
34	Full field-of-view, high-resolution, photon-counting detector CT: technical assessment and initial patient experience. Physics in Medicine and Biology, 2021, 66, 205019.	3.0	54
35	Evaluating a Convolutional Neural Network Noise Reduction Method When Applied to CT Images Reconstructed Differently Than Training Data. Journal of Computer Assisted Tomography, 2021, 45, 544-551.	0.9	17
36	Reader Performance as a Function of Patient Size for the Detection of Hepatic Metastases. Journal of Computer Assisted Tomography, 2021, Publish Ahead of Print, 812-819.	0.9	0

#	Article	IF	CITATIONS
37	CT Noise-Reduction Methods for Lower-Dose Scanning: Strengths and Weaknesses of Iterative Reconstruction Algorithms and New Techniques. Radiographics, 2021, 41, 1493-1508.	3.3	41
38	An interactive eyeâ€ŧracking system for measuring radiologists' visual fixations in volumetric CT images: Implementation and initial eyeâ€ŧracking accuracy validation. Medical Physics, 2021, 48, 6710-6723.	3.0	4
39	A Pilot Study to Estimate the Impact of High Matrix Image Reconstruction on Chest Computed Tomography. Journal of Clinical Imaging Science, 2021, 11, 52.	1.1	4
40	Optimizing Web-Based Viewer of 4D CT Scans for Clinical Assessment of Injured Wrists. , 2021, 2021, 2405-2408.		0
41	Synthesizing images from multiple kernels using a deep convolutional neural network. Medical Physics, 2020, 47, 422-430.	3.0	26
42	Dose Reduction for Sinus and Temporal Bone Imaging Using Photon-Counting Detector CT With an Additional Tin Filter. Investigative Radiology, 2020, 55, 91-100.	6.2	86
43	Electrocardiogram-Gated Computed Tomography with Coronary Angiography for Cardiac Substructure Delineation and Sparing in Patients with Mediastinal Lymphomas Treated with Radiation Therapy. Practical Radiation Oncology, 2020, 10, 104-111.	2.1	8
44	Observer Performance for Detection of Pulmonary Nodules at Chest CT over a Large Range of Radiation Dose Levels. Radiology, 2020, 297, 699-707.	7.3	15
45	Deepâ€learningâ€based direct inversion for material decomposition. Medical Physics, 2020, 47, 6294-6309.	3.0	26
46	Update on Multienergy CT: Physics, Principles, and Applications. Radiographics, 2020, 40, 1284-1308.	3.3	66
47	Multiâ€energy computed tomography and material quantification: Current barriers and opportunities for advancement. Medical Physics, 2020, 47, 3752-3771.	3.0	14
48	Quantitative Knee Arthrography in a Large Animal Model of Osteoarthritis Using Photon-Counting Detector CT. Investigative Radiology, 2020, 55, 349-356.	6.2	22
49	Multi-energy CT imaging for large patients using dual-source photon-counting detector CT. Physics in Medicine and Biology, 2020, 65, 17NT01.	3.0	14
50	Dynamic computed tomographic assessment of the mitral annulus in patients with and without mitral prolapse. Journal of Cardiovascular Computed Tomography, 2020, 14, 502-509.	1.3	7
51	A Universal Protocol for Abdominal CT Examinations Performed on a Photon-Counting Detector CT System. Investigative Radiology, 2020, 55, 226-232.	6.2	24
52	Noise reduction in CT image using prior knowledge aware iterative denoising. Physics in Medicine and Biology, 2020, , .	3.0	6
53	Deep-learning-based model observer for a lung nodule detection task in computed tomography. Journal of Medical Imaging, 2020, 7, 1.	1.5	9
54	Reducing Heart Dose with Protons and Cardiac Substructure Sparing for Mediastinal Lymphoma Treatment. International Journal of Particle Therapy, 2020, 7, 1-12.	1.8	8

#	Article	IF	CITATIONS
55	A Blooming correction technique for improved vasa vasorum detection using an ultra-high-resolution photon-counting detector CT. , 2020, 11312, .		3
56	Overcoming calcium blooming and improving the quantification accuracy of percent area luminal stenosis by material decomposition of multi-energy computed tomography datasets. Journal of Medical Imaging, 2020, 7, 053501.	1.5	5
57	Performance evaluation of computed tomography systems: Summary of AAPM Task Group 233. Medical Physics, 2019, 46, e735-e756.	3.0	148
58	Reducing radiation dose for multi-phase contrast-enhanced dual energy renal CT: pilot study evaluating prior iterative reconstruction. Abdominal Radiology, 2019, 44, 3350-3358.	2.1	4
59	Feasibility of multi ontrast imaging on dualâ€source photon counting detector (PCD) CT: An initial phantom study. Medical Physics, 2019, 46, 4105-4115.	3.0	41
60	Clinical utility of virtual noncalcium dual-energy CT in imaging of the pelvis and hip. Skeletal Radiology, 2019, 48, 1833-1842.	2.0	6
61	Dual-Energy CT Monitoring of Cryoablation Zone Growth in the Spinal Column and Bony Pelvis: A Laboratory Study. Journal of Vascular and Interventional Radiology, 2019, 30, 1496-1503.	0.5	9
62	Photon-counting Detector CT: System Design and Clinical Applications of an Emerging Technology. Radiographics, 2019, 39, 729-743.	3.3	270
63	Localization of liver lesions in abdominal CT imaging: I. Correlation of human observer performance between anatomical and uniform backgrounds. Physics in Medicine and Biology, 2019, 64, 105011.	3.0	9
64	Dual-source photon counting detector CT with a tin filter: a phantom study on iodine quantification performance. Physics in Medicine and Biology, 2019, 64, 115019.	3.0	18
65	Localization of liver lesions in abdominal CT imaging: II. Mathematical model observer performance correlates with human observer performance for localization of liver lesions in abdominal CT imaging. Physics in Medicine and Biology, 2019, 64, 105012.	3.0	8
66	A deep learning―and partial least square regressionâ€based model observer for a lowâ€contrast lesion detection task in CT. Medical Physics, 2019, 46, 2052-2063.	3.0	27
67	Improving iodine contrast to noise ratio using virtual monoenergetic imaging and prior-knowledge-aware iterative denoising (mono-PKAID). Physics in Medicine and Biology, 2019, 64, 105014.	3.0	19
68	Ability of Dual-Energy CT to Detect Silicone Gel Breast Implant Rupture and Nodal Silicone Spread. American Journal of Roentgenology, 2019, 212, 933-942.	2.2	15
69	Evaluation of Lower-Dose Spiral Head CT for Detection of Intracranial Findings Causing Neurologic Deficits. American Journal of Neuroradiology, 2019, 40, 1855-1863.	2.4	9
70	State-of-the-Art Dual-Energy Computed Tomography in Gastrointestinal and Genitourinary Imaging. Advances in Clinical Radiology, 2019, 1, 1-17.	0.2	1
71	High-Resolution Chest Computed Tomography Imaging of the Lungs. Investigative Radiology, 2019, 54, 129-137.	6.2	106
72	Reduction of Metal Artifacts and Improvement in Dose Efficiency Using Photon-Counting Detector Computed Tomography and Tin Filtration. Investigative Radiology, 2019, 54, 204-211.	6.2	76

#	Article	IF	CITATIONS
73	Impact of Effective Detector Pixel and CT Voxel Size on Accurate Estimation of Blood Volume in Opacified Microvasculature. Academic Radiology, 2019, 26, 1410-1416.	2.5	5
74	Determination of iodine detectability in different types of multiple-energy images for a photon-counting detector computed tomography system. Journal of Medical Imaging, 2019, 6, 1.	1.5	3
75	Simulation of CT images reconstructed with different kernels using a convolutional neural network and its implications for efficient CT workflow. , 2019, , .		6
76	Correlation between a deep-learning-based model observer and human observer for a realistic lung nodule localization task in chest CT. , 2019, , .		3
77	Multi-contrast imaging on dual-source photon-counting-detector (PCD) CT. , 2019, , .		3
78	Characterization of Urinary Stone Composition by Use of Whole-body, Photon-counting Detector CT. Academic Radiology, 2018, 25, 1270-1276.	2.5	17
79	Low kV versus dual-energy virtual monoenergetic CT imaging for proven liver lesions: what are the advantages and trade-offs in conspicuity and image quality? A pilot study. Abdominal Radiology, 2018, 43, 1404-1412.	2.1	30
80	Concern about a recently published paper in the European Journal of Radiology. European Journal of Radiology, 2018, 109, 203.	2.6	0
81	Comparison of a Photon-Counting-Detector CT with an Energy-Integrating-Detector CT for Temporal Bone Imaging: A Cadaveric Study. American Journal of Neuroradiology, 2018, 39, 1733-1738.	2.4	69
82	Observer Performance with Varying Radiation Dose and Reconstruction Methods for Detection of Hepatic Metastases. Radiology, 2018, 289, 455-464.	7.3	40
83	Detection and Characterization of Renal Stones by Using Photon-Counting–based CT. Radiology, 2018, 289, 436-442.	7.3	43
84	Radiation Dose in CT–guided Interventional Procedures: Establishing a Benchmark. Radiology, 2018, 289, 158-159.	7.3	3
85	Evaluation of projection―and dualâ€energyâ€based methods for metal artifact reduction in <scp>CT</scp> using a phantom study. Journal of Applied Clinical Medical Physics, 2018, 19, 252-260.	1.9	27
86	Material decomposition with prior knowledge aware iterative denoising (MD-PKAID). Physics in Medicine and Biology, 2018, 63, 195003.	3.0	39
87	150-μm Spatial Resolution Using Photon-Counting Detector Computed Tomography Technology. Investigative Radiology, 2018, 53, 655-662.	6.2	137
88	Dual-source multienergy CT with triple or quadruple x-ray beams. Journal of Medical Imaging, 2018, 5, 1.	1.5	14
89	Evaluation of a photon counting Medipix3RX cadmium zinc telluride spectral x-ray detector. Journal of Medical Imaging, 2018, 5, 1.	1.5	4
90	Ultra-high resolution photon-counting detector CT reconstruction using spectral prior image constrained compressed-sensing (UHR-SPICCS). , 2018, 10573, .		7

#	Article	IF	CITATIONS
91	Determination of optimal image type and lowest detectable concentration for iodine detection on a photon counting detector-based multi-energy CT system. , 2018, 10573, .		6
92	Impact of photon counting detector technology on kV selection and diagnostic workflow in CT. , 2018, 10573, .		10
93	Correlation between model observers in uniform background and human observer in patient liver background for a low-contrast detection task in CT. , 2018, 10577, .		2
94	An effective noise reduction method for multiâ€energy <scp>CT</scp> images that exploit spatioâ€spectral features. Medical Physics, 2017, 44, 1610-1623.	3.0	37
95	Detection of increased vasa vasorum in artery walls: improving CT number accuracy using image deconvolution. , 2017, 10132, .		1
96	Selection of optimal tube potential settings for dual-energy CT virtual mono-energetic imaging of iodine in the abdomen. Abdominal Radiology, 2017, 42, 2289-2296.	2.1	14
97	A virtual clinical trial using projection-based nodule insertion to determine radiologist reader performance in lung cancer screening CT. , 2017, 10132, .		6
98	Consistency of Renal Stone Volume Measurements Across CT Scanner Model and Reconstruction Algorithm Configurations. American Journal of Roentgenology, 2017, 209, 116-121.	2.2	5
99	A multi-reader inÂvitro study using porcine kidneys to determine the impact of integrated circuit detectors and iterative reconstruction on the detection accuracy, size measurement, and radiation dose for small (<4 mm) renal stones. Acta Radiologica, 2017, 58, 1012-1019.	1.1	2
100	Estimating patient dose from CT exams that use automatic exposure control: Development and validation of methods to accurately estimate tube current values. Medical Physics, 2017, 44, 4262-4275.	3.0	27
101	Anatomic modeling using 3D printing: quality assurance and optimization. 3D Printing in Medicine, 2017, 3, 6.	3.1	83
102	Correlation between a 2D channelized Hotelling observer and human observers in a lowâ€contrast detection task with multislice reading in <scp>CT</scp> . Medical Physics, 2017, 44, 3990-3999.	3.0	37
103	Evaluation of a projection-domain lung nodule insertion technique in thoracic computed tomography. Journal of Medical Imaging, 2017, 4, 013510.	1.5	4
104	Estimation of Observer Performance for Reduced Radiation Dose Levels in CT. Academic Radiology, 2017, 24, 876-890.	2.5	38
105	Subjective and objective heterogeneity scores for differentiating small renal masses using contrast-enhanced CT. Abdominal Radiology, 2017, 42, 1485-1492.	2.1	34
106	Utility of single-energy and dual-energy computed tomography in clot characterization: An in-vitro study. Interventional Neuroradiology, 2017, 23, 279-284.	1.1	17
107	Spectral performance of a whole-body research photon counting detector CT: quantitative accuracy in derived image sets. Physics in Medicine and Biology, 2017, 62, 7216-7232.	3.0	90
108	Estimation of signal and noise for a whole-body research photon-counting CT system. Journal of Medical Imaging, 2017, 4, 023505.	1.5	14

#	Article	IF	CITATIONS
109	Practical implementation of channelized hotelling observers: effect of ROI size. Proceedings of SPIE, 2017, 10132, .	0.8	5
110	Lowâ€dose <scp>CT</scp> for the detection and classification of metastatic liver lesions: Results of the 2016 Low Dose <scp>CT</scp> Grand Challenge. Medical Physics, 2017, 44, e339-e352.	3.0	132
111	Use of a channelized Hotelling observer to assess CT image quality and optimize dose reduction for iteratively reconstructed images. Journal of Medical Imaging, 2017, 4, 1.	1.5	9
112	Lung nodule volume quantification and shape differentiation with an ultra-high resolution technique on a photon-counting detector computed tomography system. Journal of Medical Imaging, 2017, 4, 1.	1.5	20
113	Phase-contrast imaging with a compact x-ray light source: system design. Journal of Medical Imaging, 2017, 4, 1.	1.5	1
114	Measuring arterial wall perfusion using photon-counting computed tomography (CT): improving CT number accuracy of artery wall using image deconvolution. Journal of Medical Imaging, 2017, 4, 1.	1.5	7
115	How Low Can We Go in Radiation Dose for the Data-Completion Scan on a Research Whole-Body Photon-Counting Computed Tomography System. Journal of Computer Assisted Tomography, 2016, 40, 663-670.	0.9	47
116	An open library of CT patient projection data. Proceedings of SPIE, 2016, 9783, .	0.8	7
117	Dual-source multi-energy CT with triple or quadruple x-ray beams. , 2016, 9783, .		10
118	Estimation of signal and noise for a whole-body photon counting research CT system. Proceedings of SPIE, 2016, 9783, .	0.8	4
119	Arterial wall perfusion measured with photon counting spectral x-ray CT. Proceedings of SPIE, 2016, 9967, .	0.8	12
120	Implementation and evaluation of a protocol management system for automated review of CT protocols. Journal of Applied Clinical Medical Physics, 2016, 17, 523-533.	1.9	11
121	Technical Note: Display window setting: An important factor for detecting subtle but clinically relevant artifacts in daily CT quality control. Medical Physics, 2016, 43, 6413-6417.	3.0	2
122	Technical Note: Improved CT number stability across patient size using dual-energy CT virtual monoenergetic imaging. Medical Physics, 2016, 43, 513-517.	3.0	36
123	Dose-efficient ultrahigh-resolution scan mode using a photon counting detector computed tomography system. Journal of Medical Imaging, 2016, 3, 043504.	1.5	105
124	Noise performance of low-dose CT: comparison between an energy integrating detector and a photon counting detector using a whole-body research photon counting CT scanner. Journal of Medical Imaging, 2016, 3, 043503.	1.5	74
125	The Role of Dynamic (4D) CT in the Detection of Scapholunate Ligament Injury. Journal of Wrist Surgery, 2016, 05, 306-310.	0.7	33
126	Impact of number of repeated scans on model observer performance for a low-contrast detection task in computed tomography. Journal of Medical Imaging, 2016, 3, 023504.	1.5	15

#	Article	IF	CITATIONS
127	Spectral prior image constrained compressed sensing (spectral PICCS) for photon-counting computed tomography. Physics in Medicine and Biology, 2016, 61, 6707-6732.	3.0	75
128	Validation of a Projection-domain Insertion of Liver Lesions into CT Images. Academic Radiology, 2016, 23, 1221-1229.	2.5	5
129	Human Imaging With Photon Counting–Based Computed Tomography at Clinical Dose Levels. Investigative Radiology, 2016, 51, 421-429.	6.2	205
130	Evaluation of a projection-domain lung nodule insertion technique in thoracic CT. , 2016, 9783, .		5
131	Construction of realistic phantoms from patient images and a commercial three-dimensional printer. Journal of Medical Imaging, 2016, 3, 033501.	1.5	28
132	Predicting detection performance with model observers: Fourier domain or spatial domain?. Proceedings of SPIE, 2016, 9783, .	0.8	4
133	Dual-Energy CT for Quantification of Urinary Stone Composition in Mixed Stones: A Phantom Study. American Journal of Roentgenology, 2016, 207, 321-329.	2.2	24
134	Dealing with Uncertainty in CT Images. Radiology, 2016, 279, 5-10.	7.3	21
135	CT negative attenuation pixel distribution and texture analysis for detection of fat in small angiomyolipoma on unenhanced CT. Abdominal Radiology, 2016, 41, 1142-1151.	2.1	22
136	Evaluation of conventional imaging performance in a research whole-body CT system with a photon-counting detector array. Physics in Medicine and Biology, 2016, 61, 1572-1595.	3.0	185
137	Relative accuracy of spin-image-based registration of partial capitate bones in 4DCT of the wrist. Computer Methods in Biomechanics and Biomedical Engineering: Imaging and Visualization, 2016, 4, 360-367.	1.9	4
138	Percutaneous Renal Tumor Ablation: Radiation Exposure During Cryoablation and Radiofrequency Ablation. CardioVascular and Interventional Radiology, 2016, 39, 233-238.	2.0	7
139	The influence of focal spot blooming on highâ€contrast spatial resolution in CT imaging. Medical Physics, 2015, 42, 6011-6020.	3.0	13
140	Technical Note: Development and validation of an open data format for CT projection data. Medical Physics, 2015, 42, 6964-6972.	3.0	25
141	A robust noise reduction technique for time resolved CT. Medical Physics, 2015, 43, 347-359.	3.0	11
142	Lesion insertion in the projection domain: Methods and initial results. Medical Physics, 2015, 42, 7034-7042.	3.0	18
143	Assessment of Low-Contrast Resolution for the American College of Radiology Computed Tomographic Accreditation Program. Journal of Computer Assisted Tomography, 2015, 39, 619-623.	0.9	12
144	Maximizing lodine Contrast-to-Noise Ratios in Abdominal CT Imaging through Use of Energy Domain Noise Reduction and Virtual Monoenergetic Dual-Energy CT. Radiology, 2015, 276, 562-570.	7.3	100

#	Article	IF	CITATIONS
145	Observer Performance in the Detection and Classification of Malignant Hepatic Nodules and Masses with CT Image-Space Denoising and Iterative Reconstruction. Radiology, 2015, 276, 465-478.	7.3	51
146	Image-based material decomposition with a general volume constraint for photon-counting CT. Proceedings of SPIE, 2015, 9412, .	0.8	24
147	Lesion insertion in projection domain for computed tomography image quality assessment. Proceedings of SPIE, 2015, 9412, .	0.8	7
148	Impact of number of repeated scans on model observer performance for a low-contrast detection task in CT. Proceedings of SPIE, 2015, 9416, .	0.8	1
149	Three-dimensional Physical Modeling: Applications and Experience at Mayo Clinic. Radiographics, 2015, 35, 1989-2006.	3.3	134
150	Characterization of Urinary Stone Composition by Use of Third-Generation Dual-Source Dual-Energy CT With Increased Spectral Separation. American Journal of Roentgenology, 2015, 205, 1203-1207.	2.2	36
151	Implementation of a channelized Hotelling observer model to assess image quality of x-ray angiography systems. Journal of Medical Imaging, 2015, 2, 015503.	1.5	17
152	A Technique for Quantifying Wrist Motion Using Four-Dimensional Computed Tomography: Approach and Validation. Journal of Biomechanical Engineering, 2015, 137, .	1.3	49
153	Small (< 4 cm) Renal Masses: Differentiation of Angiomyolipoma Without Visible Fat From Renal Cell Carcinoma Using Unenhanced and Contrast-Enhanced CT. American Journal of Roentgenology, 2015, 205, 1194-1202.	2.2	59
154	Prevalence of Extracoronary Vascular Abnormalities and Fibromuscular Dysplasia in Patients With Spontaneous Coronary Artery Dissection. American Journal of Cardiology, 2015, 115, 1672-1677.	1.6	167
155	Size-specific Dose Estimates for Chest, Abdominal, and Pelvic CT: Effect of Intrapatient Variability in Water-equivalent Diameter. Radiology, 2015, 276, 184-190.	7.3	66
156	Construction of realistic liver phantoms from patient images using 3D printer and its application in CT image quality assessment. , 2015, 2015, .		8
157	Use of Ionizing Radiation in Screening Examinations for Coronary Artery Calcium and Cancers of the Lung, Colon, and Breast. Seminars in Roentgenology, 2015, 50, 148-160.	0.6	4
158	Dual-energy CT for the diagnosis of gout: an accuracy and diagnostic yield study. Annals of the Rheumatic Diseases, 2015, 74, 1072-1077.	0.9	216
159	Feasibility of Discriminating Uric Acid From Non–Uric Acid Renal Stones Using Consecutive Spatially Registered Low- and High-Energy Scans Obtained on a Conventional CT Scanner. American Journal of Roentgenology, 2015, 204, 92-97.	2.2	37
160	Small (< 4 cm) Renal Mass: Differentiation of Oncocytoma From Renal Cell Carcinoma on Biphasic Contrast-Enhanced CT. American Journal of Roentgenology, 2015, 205, 999-1007.	2.2	66
161	Technical Note: Measuring contrast―and noiseâ€dependent spatial resolution of an iterative reconstruction method in CT using ensemble averaging. Medical Physics, 2015, 42, 2261-2267.	3.0	52
162	Radiation Dose Reduction in Dual-Energy CT: Does It Affect the Accuracy of Urinary Stone Characterization?. American Journal of Roentgenology, 2015, 205, W172-W176.	2.2	14

#	Article	IF	CITATIONS
163	Dual- and Multi-Energy CT: Principles, Technical Approaches, and Clinical Applications. Radiology, 2015, 276, 637-653.	7.3	1,092
164	Degradation of CT Low-Contrast Spatial Resolution Due to the Use of Iterative Reconstruction and Reduced Dose Levels. Radiology, 2015, 276, 499-506.	7.3	116
165	A novel application of CT angiography to detect extracoronary vascular abnormalities in patients with spontaneous coronary artery dissection. Journal of Cardiovascular Computed Tomography, 2014, 8, 189-197.	1.3	64
166	In Vivo Pilot Study Evaluating the Thumb Carpometacarpal Joint During Circumduction. Clinical Orthopaedics and Related Research, 2014, 472, 1106-1113.	1.5	38
167	Use of dual-energy CT and virtual non-calcium techniques to evaluate post-traumatic bone bruises in knees in the subacute setting. Skeletal Radiology, 2014, 43, 1289-1295.	2.0	50
168	Use of CT Dose Notification and Alert Values in Routine Clinical Practice. Journal of the American College of Radiology, 2014, 11, 450-455.	1.8	12
169	Correlation between human and model observer performance for discrimination task in CT. Physics in Medicine and Biology, 2014, 59, 3389-3404.	3.0	41
170	Reducing Image Noise in Computed Tomography (CT) Colonography. Journal of Computer Assisted Tomography, 2014, 38, 398-403.	0.9	18
171	Prediction of human observer performance in a 2â€alternative forced choice lowâ€contrast detection task using channelized Hotelling observer: Impact of radiation dose and reconstruction algorithms. Medical Physics, 2013, 40, 041908.	3.0	117
172	3D-3D registration of partial capitate bones using spin-images. Proceedings of SPIE, 2013, 8671, .	0.8	2
173	Electronic Noise in CT Detectors: Impact on Image Noise and Artifacts. American Journal of Roentgenology, 2013, 201, W626-W632.	2.2	83
174	Automatic Selection of Tube Potential for Radiation Dose Reduction in Vascular and Contrast-Enhanced Abdominopelvic CT. American Journal of Roentgenology, 2013, 201, W297-W306.	2.2	58
175	Correlation between model observer and human observer performance in CT imaging when lesion location is uncertain. Medical Physics, 2013, 40, 081908.	3.0	83
176	Individualized kV Selection and Tube Current Reduction in Excretory Phase Computed Tomography Urography. Journal of Computer Assisted Tomography, 2013, 37, 551-559.	0.9	20
177	Achieving Routine Submillisievert CT Scanning: Report from the Summit on Management of Radiation Dose in CT. Radiology, 2012, 264, 567-580.	7.3	246
178	Attenuationâ€based estimation of patient size for the purpose of size specific dose estimation in CT. Part II. Implementation on abdomen and thorax phantoms using cross sectional CT images and scanned projection radiograph images. Medical Physics, 2012, 39, 6772-6778.	3.0	67
179	Attenuationâ€based estimation of patient size for the purpose of size specific dose estimation in CT. Part I. Development and validation of methods using the CT image. Medical Physics, 2012, 39, 6764-6771.	3.0	76
180	Applications of Dual-Energy CT in Urologic Imaging: An Update. Radiologic Clinics of North America, 2012, 50, 191-205.	1.8	53

#	Article	IF	CITATIONS
181	Dual-Energy CT–Based Monochromatic Imaging. American Journal of Roentgenology, 2012, 199, S9-S15.	2.2	483
182	CT Dose Index and Patient Dose: They Are <i>Not</i> the Same Thing. Radiology, 2011, 259, 311-316.	7.3	377
183	Noise reduction in spectral CT: Reducing dose and breaking the tradeâ€off between image noise and energy bin selection. Medical Physics, 2011, 38, 4946-4957.	3.0	95
184	Radiation Dose Reduction for CT-Guided Renal Tumor Cryoablation. American Journal of Roentgenology, 2011, 196, W586-W591.	2.2	16
185	Identification of Intraarticular and Periarticular Uric Acid Crystals with Dual-Energy CT: Initial Evaluation. Radiology, 2011, 261, 516-524.	7.3	211
186	Dynamic CT technique for assessment of wrist joint instabilities. Medical Physics, 2011, 38, S50-S56.	3.0	69
187	Radiation Dose Levels for Interventional CT Procedures. American Journal of Roentgenology, 2011, 197, W97-W103.	2.2	77
188	Virtual monochromatic imaging in dualâ€source dualâ€energy CT: Radiation dose and image quality. Medical Physics, 2011, 38, 6371-6379.	3.0	282
189	Dual-Energy Dual-Source CT With Additional Spectral Filtration Can Improve the Differentiation of Non–Uric Acid Renal Stones: An Ex Vivo Phantom Study. American Journal of Roentgenology, 2011, 196, 1279-1287.	2.2	120
190	Radiation Dose Reduction at CT Enterography: How Low Can We Go While Preserving Diagnostic Accuracy?. American Journal of Roentgenology, 2010, 195, 76-77.	2.2	27
191	Imaging evaluation and treatment of nephrolithiasis: an update. Minnesota Medicine, 2010, 93, 48-51.	0.1	1
192	Radiation dose reduction in computed tomography: techniques and future perspective. Imaging in Medicine, 2009, 1, 65-84.	0.0	296
193	Dualâ€ s ource spiral CT with pitch up to 3.2 and 75 ms temporal resolution: Image reconstruction and assessment of image quality. Medical Physics, 2009, 36, 5641-5653.	3.0	155
194	Prior image constrained compressed sensing (PICCS): A method to accurately reconstruct dynamic CT images from highly undersampled projection data sets. Medical Physics, 2008, 35, 660-663.	3.0	939
195	High temporal resolution and streak-free four-dimensional cone-beam computed tomography. Physics in Medicine and Biology, 2008, 53, 5653-5673.	3.0	140
196	Streaking artifacts reduction in fourâ€dimensional coneâ€beam computed tomography. Medical Physics, 2008, 35, 4649-4659.	3.0	88
197	Exact fan-beam image reconstruction algorithm for truncated projection data acquired from an asymmetric half-size detector. Physics in Medicine and Biology, 2005, 50, 1805-1820.	3.0	28